Probing the Balance between Localization and Delocalization of the Metal-Based Electrons in Face-Shared Bioctahedral Complexes

John E. McGrady, Timothy Lovell, and Robert Stranger*

The Department of Chemistry, The Faculties, The Australian National University, Canberra, ACT 0200, Australia

Received October 7, 1996[⊗]

The electronic structures of a variety of metal nonahalides, $MM'X_9$, with the $\{d^3d^3\}$ configuration are examined using broken-symmetry density functional theory. Complexes containing trivalent ions of the chromium triad and tetravalent ions of the manganese triad are considered, where metal−metal interactions range from strong multiple bonding to weak antiferromagnetic coupling. The division of the metal-based electrons into symmetry-distinct σ and δ_π subsets also gives rise to an intermediate group of complexes, where the σ electrons are involved in a strong bond, but the δ_π subset remain weakly coupled. The balance between localization and delocalization of the metal-based electrons is determined by two distinct factors. The overlap of metal-based orbitals favors delocalization, whereas the high single-ion spin polarization energy associated with an isolated d^3 ion favors localization. Independent estimates of these two factors are made, and their contribution to the observed periodic trends is assessed. On descending a triad, the radial expansion of the d orbitals reduces the single-ion spin polarization energy and also increases overlap between orbitals on adjacent centers. Both factors contribute approximately equally to the increased tendency of the metal-based electrons to delocalize in the heavier congeners. Moving across a period, the greater covalence of the M^{IV}−Cl bond in complexes of the manganese triad reduces the spin polarization energy, favoring delocalization. The contracted orbitals of the M^{IV} ion, however, reduce the orbital overlap term, favoring localization. Changes in the overlap term dominate, and hence the overall trend is toward greater localization of the metal-based electrons in complexes of the manganese triad.

Introduction

The metal−metal bonding in confacial bioctahedral systems such as the metal nonachlorides, M_2X_9, has been described by a number of authors using extended Hückel,[1] density functional,[2] and *ab initio* techniques.[3] The qualitative features of the interaction between the metal-based orbitals are summarized in Figure 1. The local trigonal symmetry at each metal center splits the octahedral t_{2g} orbitals into symmetry-distinct subsets, a_1 and e, which have σ and δ_π symmetry with respect to the trigonal axis.[4] In the presence of weak antiferromagnetic coupling between the two metals, the orbitals remain localized on one center or the other, but as the coupling between the two centers increases, the orbitals progressively delocalize over both metal ions and bonding (σ, δ_π) and antibonding (σ^*, δ_π^*) combinations diverge to lower and higher energy, respectively. The extremes of metal−metal bonding possible within the face-sharing architecture are best illustrated by the isoelectronic pair of complexes, $Cr_2Cl_9^{3-}$ and $W_2Cl_9^{3-}$, both of which have the $\{d^3d^3\}$ configuration and hence a formal bond order of 3. The dichromium system has a very long Cr−Cr separation and is paramagnetic at room temperature,[5] indicating that the ground state corresponds to the weak antiferromagnetic coupling of two Cr^{3+} ions. In contrast, the $[W_2Cl_9]^{3-}$ ion exhibits properties characteristic of a W−W triple bond, most notably a short W−W separation and diamagnetic behavior at room temperature.[6]

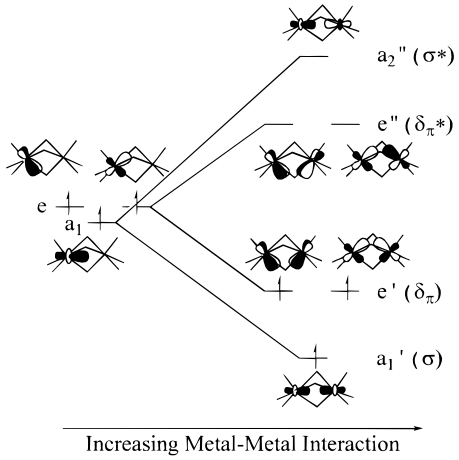

Figure 1. Energies and distributions of the metal-based orbitals of a confacial bioctahedron as a function of metal−metal interaction. Only spin-up orbitals are shown; the corresponding spin-down orbitals are related to their spin-up counterparts by reflection in a plane containing the three bridging ligands.

In order to describe the weakly coupled limit, it is clearly necessary to allow the two metal centers to behave independently, thereby permitting the localization of spin-up or spin-down electrons on one center or the other. This can be achieved in spin-unrestricted density functional theory by removing all symmetry elements connecting the two centers, corresponding to a reduction in point symmetry from D_{3h} to C_{3v} in the case of

[⊗] Abstract published in *Advance ACS Abstracts,* June 15, 1997.

(1) Summerville, R. H.; Hoffmann, R. *J. Am. Chem. Soc.* **1979**, *101*, 3821.
(2) (a) Ginsberg, A. P. *J. Am. Chem. Soc.* **1980**, *102*, 111. (b) Bursten, B. E.; Cotton, F. A.; Fang, A. *Inorg. Chem.* **1983**, *22*, 2127. (c) Gheller, S. F.; Heath, G. A.; Humphrey, D. G.; Hockless, D. C. R.; McGrady, J. E. *Inorg. Chem.* **1994**, *33*, 3986. (d) Heath, G. A.; McGrady, J. E. *J. Chem. Soc., Dalton Trans.* **1994**, 3759.
(3) Cotton, F. A.; Feng, X. *Int. J. Quantum Chem.* **1996**, *58*, 671.
(4) Trogler, W. C. *Inorg. Chem.* **1980**, *19*, 697.
(5) (a) Saillant, R.; Wentworth, R. A. D. *Inorg. Chem.* **1968**, *7*, 1606. (b) Wessel, G. J.; Ijdo, D. J. W. *Acta Crystallogr.* **1957**, *10*, 466. (c) Grey, I. E.; Smith, P. W. *Aust. J. Chem.* **1971**, *24*, 73.
(6) (a) Dunbar, K. R.; Pence, L. E. *Acta Crystallogr. C* **1991**, *47*, 23. (b) Watson, W. H., Jr.; Waser, J. *Acta Crystallogr.* **1958**, *11*, 689. (c) Stranger, R.; Smith, P. W.; Grey, I. E. *Inorg. Chem.* **1989**, *28*, 1271.

S0020-1669(96)01208-6 CCC: $14.00

the metal nonahalides. This broken-symmetry technique[7] incorporates valence bond features into the description of the metal−metal bond and has been used to provide a much improved description of weakly interacting electrons in main group[8] and transition metal systems.[9,10] It should be emphasized at this point that the broken-symmetry method does not force the electrons to localize; it merely allows them to do so if the localized situation is more stable than the corresponding delocalized one. Thus in the limit of strong metal−metal bonding, the broken-symmetry solution is identical to that obtained from a calculation in which full delocalization is enforced by the presence of symmetry elements linking the two metals. The broken-symmetry method therefore encompasses both weak antiferromagnetic coupling and strong metal−metal bonding, as well as a continuum of intermediate situations, making it an ideal tool for the study of periodic trends in metal−metal bonding.

In a recent communication we described the importance of symmetry breaking when calculating metal−metal separations in the nonachlorides, $[M_2Cl_9]^{3-}$, M = Cr, Mo, W.[11] As noted above, the W−W bond is strong, and consequently at self-consistency the metal-based electrons are delocalized. The optimized W−W separations obtained from calculations performed in full (D_{3h}) and broken (C_{3v}) symmetry are therefore identical (2.40 Å) and in excellent agreement with available structural data.[6] In contrast, the metal-based electrons are completely localized in $Cr_2Cl_9^{3-}$, and the broken-symmetry optimized structure has a long Cr−Cr separation of 3.22 Å, again in good agreement with the experimentally determined range of values.[5] However, if full delocalization is imposed by enforcing D_{3h} symmetry, the optimized Cr−Cr separation is only 2.29 Å, almost 1.0 Å shorter than the crystallographic range. Following this initial report of optimized metal−metal separations, we examined in detail the potential energy curves of the broken-symmetry states of $[Cr_2Cl_9]^{3-}$, $[Mo_2Cl_9]^{3-}$, $[W_2Cl_9]^{3-}$, and $[Re_2Cl_9]^{-}$,[12] schematic representations of which are illustrated in Figure 2. The corresponding curves for the pure singlet ground states, obtained by the approximate spin projection technique developed by Noodleman,[13] were found to closely follow the broken-symmetry states at all metal−metal separations. The potential energy curves may be divided into three distinct regions depending on which subsets of electrons are weakly antiferromagnetically coupled (localized) and which are involved in a strong metal−metal bond (delocalized). At short metal−metal separations both σ and δ_π subsets are involved in strong metal−metal bonding and hence are fully delocalized over both centers. As r(M−M) is increased, the δ_π manifold localizes before σ as a consequence of the poorer overlap of the δ_π orbitals. The combination of strong bonding within the σ subset and antiferromagnetic coupling within δ_π maintains a singlet ground state. Finally, at large r(M−M) both

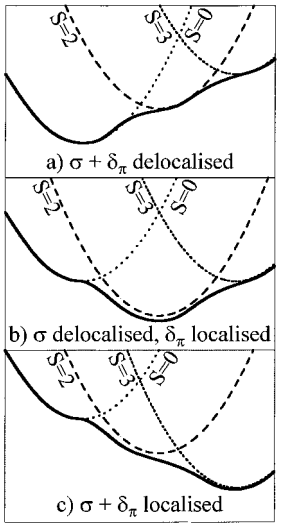

Figure 2. Schematic representation of the potential energy curves for M_2Cl_9 complexes with the $\{d^3d^3\}$ configuration.

σ and δ_π subsets localize, and the broken-symmetry state corresponds to weak antiferromagnetic coupling of both σ and δ_π manifolds.

The three distinct sections of the curve can be identified most easily by considering three associated pure spin states, each calculated using full D_{3h} symmetry (Figure 2). The spin singlet associated state ($S = 0$), $(a_1'\uparrow)^1(a_1'\downarrow)^1(e'\uparrow)^2(e'\downarrow)^2(e''\uparrow)^0(e''\downarrow)^0(a_2''\uparrow)^0(a_2''\downarrow)^0$, corresponds precisely to the full-symmetry calculation described above and has a net metal−metal bond order of 3. In contrast, the $S = 3$ associated state, which arises from the spin-unrestricted $(a_1'\uparrow)^1(a_1'\downarrow)^0(e'\uparrow)^2(e'\downarrow)^0(e''\uparrow)^2(e''\downarrow)^0(a_2''\uparrow)^1(a_2''\downarrow)^0$ configuration, has a bond order of 0, and an excess of six spin-up electrons, three per metal center. This state therefore corresponds to the ferromagnetic coupling of all six metal-based electrons. In the intermediate $S = 2$ state, $(a_1'\uparrow)^1(a_1'\downarrow)^1(e'\uparrow)^2(e'\downarrow)^0(e''\uparrow)^2(e''\downarrow)^0(a_2''\uparrow)^0(a_2''\downarrow)^0$, the σ electrons are antiferromagnetically coupled, but ferromagnetic coupling prevails within the δ_π manifold, resulting in a bond order of 1. The $S = 1$ state, corresponding to uncoupling of only one of the pairs of δ_π electrons, cannot be represented by a single determinant wavefunction and consequently is not considered here.

The connection between the $S = 0$, 2, and 3 associated states and the broken-symmetry curve can be made by noting that where overlap of a subset of metal-based orbitals is weak, states corresponding to ferromagnetic and antiferromagnetic coupling of the electrons within these orbitals will lie close in energy. Therefore at large r(M−M), where overlap of both σ and δ_π orbitals is minimal, the $S = 3$ state lies close to the broken-symmetry curve (within 0.05 eV), indicating that both σ and δ_π subsets of electrons are weakly antiferromagnetically coupled in the latter. At shorter separations, where the σ orbitals are delocalized and only the δ_π subset remains weakly antiferromagnetically coupled, the $S = 2$ curve, corresponding to ferromagnetic coupling of only the δ_π electrons, approaches the broken-symmetry curve. Finally, at even shorter separations, all metal-based electrons delocalize, and the broken-symmetry solution converges with the $S = 0$ state. The broken-symmetry curve therefore follows the path of lowest energy between the three pure spin states, making a smooth transition from one region to the next where the curves intersect. The ground-state properties of any particular system are therefore determined by the minimum energies of the three associated states, $S = 0$, 2, and 3. Where the $S = 0$ state lies lower than either $S = 2$ or $S = 3$, all electrons are delocalized, resulting in a metal−metal triple bond, and the metal−metal separation is correspondingly short (Figure 2a). At the opposite extreme, if $S = 3$ lies lowest,

(7) Noodleman, L.; Norman, J. G., Jr. *J. Chem. Phys.* **1979**, *70*, 4903.
(8) Andzelm, J.; Wimmer, E. *J. Chem. Phys.* **1992**, *96*, 1280.
(9) (a) Delley, B.; Freeman, A. J.; Ellis, D. E. *Phys. Rev. Lett.* **1985**, *54*, 661. (b) Baykara, N. A.; McMaster, B. N.; Salahub, D. R. *Mol. Phys.* **1984**, *52*, 891. Dunlap, B. I. *Phys. Rev. A* **1983**, *27*, 2217.
(10) (a) Bencini, A.; Gatteschi, D. *J. Am. Chem. Soc.* **1986**, *108*, 5763. (b) Aizman, A.; Case, D. A. *J. Am. Chem. Soc.* **1982**, *104*, 3269. (c) Ross, P. K.; Solomon, E. I. *J. Am. Chem. Soc.* **1991**, *113*, 3246. (d) Noodleman, L.; Case, D. A. *Adv. Inorg. Chem.* **1992**, *38*, 423. (e) Mouesca, J.-M.; Chen, J. L.; Noodleman, L.; Bashford, D.; Case, D. A. *J. Am. Chem. Soc.* **1994**, *116*, 11898. (f) Brown, C. A.; Remar, G. J.; Musselman, R. L.; Solomon, E. I. *Inorg. Chem.* **1995**, *34*, 688. (g) Medley, G. A.; Stranger, R. *Inorg. Chem.* **1994**, *33*, 3976.
(11) Lovell, T.; McGrady, J. E.; Stranger, R.; MacGregor, S. A. *Inorg. Chem.* **1996**, *35*, 3079.
(12) McGrady, J. E.; Stranger, R.; Lovell, T. Submitted to *J. Phys. Chem.*, manuscript no. JP9625568.
(13) (a) Noodleman, L. *J. Chem. Phys.* **1981**, *74*, 5737. (b) Edgecombe. K. E.; Becke, A. D. *Chem. Phys. Lett.* **1995**, *244*, 427.

all metal-based electrons are localized, no significant metal−metal bonding arises, and the metal−metal separation is large (Figure 2c). Where $S = 2$ lies lowest (Figure 2b), only an effective metal−metal σ bond is present in the ground state, and the optimized bond length consequently takes an intermediate value.

In this paper, we use the relative energies of the associated spin states, $S = 0$, 2, and 3, to explore the electronic and structural properties of a wider range of metal nonachlorides with the $\{d^3d^3\}$ configuration. In particular, we aim to identify the properties of the individual metal ions which determine whether the electrons are localized or delocalized in the dimer, and how these factors vary across the periodic table. Optimized structures and relative energies of the broken-symmetry, $S = 0$, $S = 2$, and $S = 3$ states of the M_2Cl_9 ($M = Cr^{3+}$, Mo^{3+}, W^{3+}, Mn^{4+}, Tc^{4+} and Re^{4+}) complexes are presented, along with those of the mixed-metal systems $[CrMoCl_9]^{3-}$, $[MoWCl_9]^{3-}$, $[MnTcCl_9]^{-}$, and $[TcReCl_9]^{-}$. Of the homonuclear systems, $[Mn_2Cl_9]^{-}$ and $[Tc_2Cl_9]^{-}$ are as yet unknown, although $Tc_2Br_9^{-}$ has recently been synthesized.[14] The heteronuclear systems $[MM'Cl_9]^{3-}$ have received less attention in the literature, but the CrMo complex $[CrMoCl_9]^{3-}$ has been synthesized,[15] and its magnetic moment is reported to be intermediate between those of $[Cr_2Cl_9]^{3-}$ and $[Mo_2Cl_9]^{3-}$. Attempts to prepare the other mixed-metal complexes have as yet been unsuccessful, although the hydride-bridged species $[MoWCl_8H]^{3-}$ has been structurally characterized and found to have a MoW separation of 2.445(3) Å,[16] significantly longer than that observed in the homonuclear analogue $[Mo_2Cl_8H]^{3-}$ [2.38(1) Å].[17] This trend contrasts with that in the acetate-bridged complexes, $M_2(O_2CR)_4$, where the metal−metal separation in $MoW(O_2CCH_3)_4$ [2.080(1) Å][16,18] is less than that in either $Mo_2(O_2CCH_3)_4$ [2.093(1) Å][19] or $W_2(O_2CC_2H_5)_4$ [2.189(1) Å].[20] Thus it appears that the heteronuclear character of a complex can result in either shorter or longer metal−metal separations compared to those of its homonuclear neighbors, depending on the ligand environment. Both the acetate- and the hydride-bridged species described above are forced to adopt relatively short metal−metal separations, the former by the presence of four bridging acetate groups, the latter by the small bridging hydride. In contrast, the wide range of metal−metal separations found in confacial bioctahedral systems[21] suggests that the μ-Cl_3 moiety is a very flexible bridging group. Consequently, we anticipate that the triple halide bridge will allow the structure of the dimer to be determined largely by the electronic properties of the component metal ions rather than the steric constraints of the bridge.

Computational Details

All calculations described in this work were performed on either IBM RISC6000 or SunUltraSparc 170/140 workstations using the Amsterdam Density Functional (ADF) program version 2.0.1 developed by Baerends *et al.*[22] The local density approximation (LDA) to the exchange potential was used,[23] along with the correlation potential of Vosko, Wilk, and Nusair.[24] The influence of gradient[25] and quasi-relativistic corrections[26] to the LDA were examined in detail in a previous paper[12] and found to provide generally poorer agreement with crystallographically determined structural parameters than the LDA in isolation. Accordingly, neither correction is included in the present study. A double-ζ Slater type orbital basis set extended with a single d-polarization function was used to describe the main group atoms, while all metals were modeled with triple-ζ basis sets.[27] Electrons in orbitals up to and including 2p {Cl}, 3p {Cr, Mn}, 4p {Mo, Tc}, and 5p {W, Re} were considered to be part of the core and treated in accordance with the frozen-core approximation. Geometries were optimized using the algorithm of Versluis and Ziegler.[28] The full D_{3h} point symmetry of the confacial bioctahedron was used when the energy of the associated $S = 0$, 2, and 3 states was calculated. For the broken-symmetry calculations, all symmetry elements connecting the two metal centers were removed, resulting in overall C_{3v} symmetry. Approximate spin-projection of the broken-symmetry state is not performed here, as the resultant pure singlet ground state has been found to closely follow the broken-symmetry curve at all points.[12] Calculations on the heteronuclear systems $MM'Cl_9^{3-}$ were performed in C_{3v} symmetry, and those on the monomeric hexahalides, $[MCl_6]$,$^{3-/2-}$ were performed in O_h symmetry. Spin-restricted calculations on the hexachlorides correspond to a d orbital occupation of $(t_{2g}^{\uparrow})^{1.5}(t_{2g}^{\downarrow})^{1.5}$, while unrestricted calculations were performed using $(t_{2g}^{\uparrow})^{3.0}(t_{2g}^{\downarrow})^{0.0}$. M−Cl bond lengths were independently optimized in each case.

Table 1. Metal−Metal Separations, r(M−M) (Å), for the Various States of M_2Cl_9 Complexes[a]

		$S = 0$	$S = 2$	$S = 3$	ref state	broken sym
$[Cr_2Cl_9]^{3-}$	r(M−M)/Å	2.29	2.78	3.25	3.23	3.22
	(E_{rel}/eV)	(0.00)	(−1.46)	(−2.53)	(+1.02)	(−2.53)
$[CrMoCl_9]^{3-}$		2.27	2.87	3.35	3.34	3.27
		(0.00)	(−0.58)	(−0.98)	(+1.90)	(−1.00)
$[Mo_2Cl_9]^{3-}$		2.29	2.87	3.46	3.45	2.29
		(0.00)	(+0.41)	(+0.69)	(+2.88)	(0.00)
$[MoWCl_9]^{3-}$		2.35	2.91	3.51	3.50	2.35
		(0.00)	(+0.52)	(0.90)	(+2.99)	(0.00)
$[W_2Cl_9]^{3-}$		2.40	2.91	3.52	3.52	2.40
		(0.00)	(+0.61)	(+1.10)	(+3.10)	(0.00)
$[Mn_2Cl_9]^{-}$		2.46	2.82	3.13	3.13	3.14
		(0.00)	(−1.56)	(−2.81)	(+0.17)	(−2.81)
$[MnTcCl_9]^{-}$		2.40	3.10	3.20	3.20	3.19
		(0.00)	(−1.05)	(−1.50)	(+0.84)	(−1.51)
$[Tc_2Cl_9]^{-}$		2.43	2.79	3.29	3.28	2.87
		(0.00)	(−0.22)	(−0.20)	(+1.69)	(−0.30)
$[TcReCl_9]^{-}$		2.45	2.82	3.32	3.31	2.82
		(0.00)	(−0.08)	(+0.18)	(+1.69)	(−0.15)
$[Re_2Cl_9]^{-}$		2.49	2.85	3.36	3.35	2.79
		(0.00)	(+0.03)	(+0.31)	(+1.85)	(−0.04)

[a] Total energies, E_{rel} (eV), relative to the $S = 0$ state, are given in parentheses.

Results and Discussion

Optimized metal−metal separations for the various states of all 10 complexes are summarized in Table 1. Total energies, relative to the $S = 0$ state in each case, are given in parentheses and are plotted in Figure 3. In all cases the mixed-metal systems lie approximately midway between their homonuclear counterparts, and the relative energies of the spin states form a

(14) Preetz, W.; Wendt, A. *Z. Anorg. Allg. Chem.* **1993**, *619*, 1669.
(15) Matson, M. S.; Wentworth, R. A. D. *J. Am. Chem. Soc.* **1974**, *96*, 7837.
(16) Katovic, V.; McCarley, R. E. *J. Am. Chem. Soc.* **1978**, *100*, 5586.
(17) Bennet, M. J.; Brencic, J. V.; Cotton. F. A. *Inorg. Chem.* **1969**, *8*, 1060.
(18) Robbins, G. A.; Martin, D. S. *Inorg. Chem.* **1984**, *23*, 2086.
(19) Kepert, D. L.; Skelton, B. W.; White, A. H. *Aust. J. Chem.* **1980**, *33*, 1847.
(20) Chisholm, M. H.; Chiu, H. T.; Huffman, J. C. *Polyhedron* **1984**, *3*, 759.
(21) Cotton, F. A.; Ucko, D. A. *Inorg. Chim. Acta* **1972**, *6*, 161.
(22) The Amsterdam Density Functional Program, see (a) Baerends, E. J.; Ellis, D. E.; Ros, P. *Chem. Phys.* **1973**, *2*, 42. (b) Baerends, E. J.; Ros, P. *Chem. Phys.* **1973**, *2*, 52. (c) Baerends, E. J.; Ros, P. *Int. J. Quantum Chem.* **1978**, *S12*, 169.
(23) (a) Parr, R. G.; Yang, W. *Density Functional Theory of Atoms and Molecules*; Oxford University Press: New York, 1989. (b) Ziegler, T. *Chem Rev.* **1991**, *91*, 651.
(24) Vosko, S. H.; Wilk, L.; Nusair, M. *Can. J. Phys.* **1980**, *58*, 1200.
(25) (a) Becke, A. D. *Phys. Rev. A* **1988**, *38*, 3098. (b) Perdew, J. P. *Phys. Rev. B* **1986**, *33*, 8822. (c) Perdew, J. P.; Chekavry, J. A.; Vosko, S. H.; Jackson, K. A.; Pederson, M. R.; Singh, D. J.; Fioihais, C. *Phys. Rev. B* **1992**, *46*, 6671.
(26) Ziegler, T.; Baerends, E. J.; Snijders, J. G.; Ravenek, W. *J. Phys. Chem.* **1989**, *93*, 3050.
(27) Vernooijs, P.; Snijders, G. L.; Baerends, E. J. Slater Type Basis Functions for the Whole Periodic Table. Internal Report, Vrije Universiteit: Amsterdam, 1981.
(28) Versluis, L.; Ziegler, T. *J. Chem. Phys.* **1988**, *88*, 322.

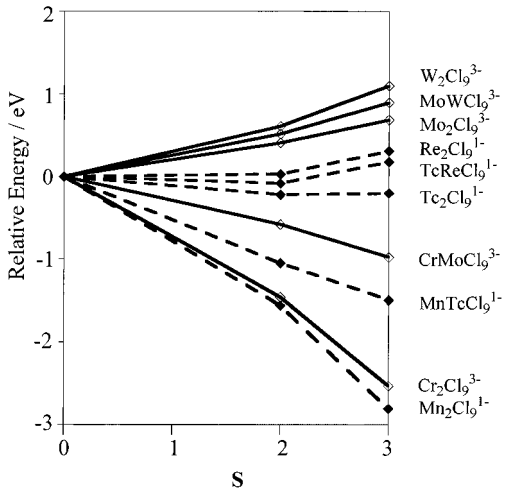

Figure 3. Relative energies of the associated $S = 0$, 2, and 3 states for M_2Cl_9 complexes.

continuous spectrum from $[Mn_2Cl_9]^-$ at one extreme to $[W_2Cl_9]^{3-}$ at the other. This observation suggests that in systems such as the metal nonahalides, where the bridging architecture is very flexible, the electronic structure of the dimer is determined by the sum of the contributions of the isolated single ions. The intermediate position of the mixed-metal species is not, however, expressed in the calculated ground-state structures of the molecules. The optimized metal−metal separations of the broken-symmetry states (shown in Table 1) fall into three narrow bands: short (2.35 ± 0.06 Å), intermediate (2.83 ± 0.04 Å), and long (3.21 ± 0.07 Å). The absence of a continuum of metal−metal separations is linked to the shape of the potential energy surfaces shown in Figure 2. The equilibrium metal−metal separation is determined not by the separation of the various spin states but simply by which lies lowest. The data in Table 1 indicate that the values of r(M−M) at the minima in the three pure spin states are relatively insensitive to the changes in the metal ion (2.38 ± 0.11 Å, 2.94 ± 0.16 Å, and 3.32 ± 0.20 Å for $S = 0$, 2, and 3, respectively). The three distinct regions of the broken-symmetry curve therefore occur over approximately the same range of metal−metal separations, regardless of the identity of the metal ion. In contrast, the relative energies of the associated states vary greatly, and when a reversal in the ordering occurs, the position of the global minimum in the broken-symmetry curve switches abruptly from one region to the next, rather than taking on a continuum of values (Figure 2). It is important at this stage to distinguish between the optimized metal−metal separations shown in Table 1 and their crystallographically determined counterparts. The optimized metal−metal separation corresponds to an isolated molecule at 0 K in the gas phase, where only the ground state is populated. The experimental data, in contrast, refer to measurements made in the solid state at ambient temperatures, where thermal motion or the presence of counterions may force the anion away from the global minimum in the gas-phase potential energy curve. The extent to which the crystalline environment can force a change in the metal−metal separation is clearly related to the depth of the minimum in the potential energy curve, which in turn is related to the separation of the associated spin states. The closer in energy the states lie, the flatter the broken-symmetry potential energy curve, and hence the wider the range of accessible metal−metal separations. In summary, the position of the minimum in the calculated broken-symmetry potential energy curve is dictated solely by which spin state lies lowest, but the experimentally accessible range of values depends on the shape of the curve, and hence on the relative energies of the spin states.

The complexes of the chromium triad separate clearly into two distinct groups: those in which the $S = 3$ state is most stable ($[Cr_2Cl_9]^{3-}$, $[CrMoCl_9]^{3-}$) and those in which $S = 0$ is most stable ($[Mo_2Cl_9]^{3-}$, $[MoWCl_9]^{3-}$, $[W_2Cl_9]^{3-}$). Thus at equilibrium, the broken-symmetry ground states of $[Cr_2Cl_9]^{3-}$ and $[CrMoCl_9]^{3-}$ have fully localized electrons and long metal−metal separations, whereas the electrons in the heavier complexes are fully delocalized and metal−metal separations are short. These observations are consistent with the known structural and magnetic properties of $[Cr_2Cl_9]^{3-}$, $[CrMoCl_9]^{3-}$, and $[W_2Cl_9]^{3-}$, but not for $[Mo_2Cl_9]^{3-}$, where the Mo−Mo separation varies from 2.53 to 2.78 Å depending on the size of the countercation.[6c,29] We note from Table 1 that the three pure spin states lie closer together for $[Mo_2Cl_9]^{3-}$ than for either $[Cr_2Cl_9]^{3-}$ or $[W_2Cl_9]^{3-}$. As a consequence, population of the higher spin states, induced either thermally or by environmental factors, may be sufficiently large to force the anion away from the global minimum at r(Mo−Mo) = 2.29 Å. This possibility has been discussed in detail elsewhere.[12]

The tetravalent complexes of the manganese triad show similar trends, but the higher spin states are uniformly stabilized relative to $S = 0$. This shift does not alter the identity of the lowest lying state ($S = 3$) for the lighter complexes ($[Mn_2Cl_9]^-$, $[MnTcCl_9]^-$), which therefore have ground-state properties very similar to those of their counterparts in the chromium triad (localized electrons, long r(M−M)). For the heavier complexes, however, all three spin states now lie close together, indicating that the equilibrium between localization and delocalization is delicately balanced. For the dirhenium system, $[Re_2Cl_9]^-$, the energies of the states increase in the order $S = 0 \approx S = 2 < S = 3$, and hence in the broken-symmetry ground state, the σ electrons are delocalized but the δ_π manifold remains localized (Figure 2b). The optimized metal−metal separation therefore takes on an intermediate value of 2.79 Å, in very good agreement with the crystallographically determined value of 2.71 Å.[30] The proximity of the $S = 0$ state, however, suggests that delocalization of the δ_π electrons will be a relatively facile process, and environmental factors may cause a contraction of the Re−Re bond. In the technetium system, $[Tc_2Cl_9]^-$, the ordering of states is $S = 3 \approx S = 2 < S = 0$, and once again only the σ electrons are delocalized in the broken-symmetry ground state. In this case, however, the next lowest state is $S = 3$ (as opposed to $S = 0$ for the rhenium analogue), indicating that localization of the σ electrons is more likely to occur than delocalization of the δ_π manifold. Thus, although the optimized M−M separations in $[Re_2Cl_9]^-$ and $[Tc_2Cl_9]^-$ are very similar, the former lies close to the borderline with full delocalization, while the latter lies near the fully localized regime. The responses of the anions to environmental changes are likely to reflect this difference, with Re−Re separations shorter than 2.79 Å and Tc−Tc separations longer than 2.87 Å being accessible.

Having established the periodic trends in the relative stabilities of the associated states, we now proceed to analyze these trends in terms of the fundamental electronic properties of the component metal ions. Two factors influence the extent to which metal-based electrons delocalize in a bimetallic system. Firstly, significant overlap of the orbitals on the two centers will favor delocalization of the metal-based electrons. A second, more subtle effect involves the loss of spin polarization energy on each metal center as the electrons delocalize.[9a,31] In the limit of full localization, each single ion has three metal-based

(29) (a) Stranger, R.; Grey, I. E.; Madsen, I. C.; Smith, P. W. *J. Solid State Chem.* **1987**, *69*, 162. (b) Saillant, R.; Jackson, R. B.; Streib, W.; Folting, K.; Wentworth, R. A. D. *Inorg. Chem.* **1971**, *10*, 1453.
(30) Heath, G. A.; McGrady, J. E.; Raptis, R. G.; Willis, A. C. *Inorg. Chem.* **1996**, *35*, 6838.

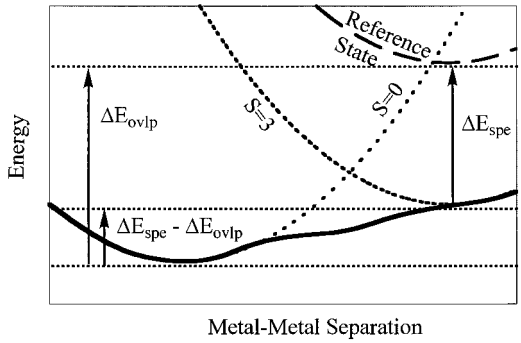

Figure 4. Schematic representation of the $S = 0$, $S = 3$, and reference states and the terms ΔE_{ovlp} and ΔE_{spe}.

electrons, coupled in parallel, in accordance with Hund's rule. The localized broken-symmetry state is therefore stabilized by the spin polarization energy associated with the presence of three spin-up electrons on one center and three spin-down electrons on the other. The delocalization of these electrons is accompanied by a reduction in the unpaired spin density on each metal ion, and hence in the single-ion spin polarization energy. The transition from localized to delocalized regimes will therefore occur only when the energy gain associated with orbital overlap can overcome the loss of single-ion spin polarization energy. Qualitatively, we anticipate that increasing the size of the metal ions will enhance metal−metal overlap, and also reduce spin polarization energy by increasing the average separation between the electrons. These two factors, increasing orbital overlap and decreasing spin polarization energy, both favor delocalization in the complexes of the heavier metals. Our aim here is to separate the contributions of these two factors and determine whether changes in one or the other dominate the observed periodic trends.

The concept of separate orbital overlap and spin polarization terms can be connected with the states shown in Figure 2 by noting that the $S = 0$ state $[(a_1'\uparrow)^1(a_1'\downarrow)^1(e'\uparrow)^2(e'\downarrow)^2(e''\uparrow)^0(e''\downarrow)^0(a_2''\uparrow)^0(a_2''\downarrow)^0]$ has a metal−metal triple bond, but no spin polarization energy. In contrast, the $S = 3$ state, $[(a_1'\uparrow)^1(a_1'\downarrow)^0(e'\uparrow)^2(e'\downarrow)^0(e''\uparrow)^2(e''\downarrow)^0(a_2''\uparrow)^1(a_2''\downarrow)^0]$, has no net metal−metal bond, but has an excess of three electrons per metal center, and hence is stabilized by spin polarization only. Thus we can equate the depth of the $S = 0$ curve with the energetic contribution of orbital overlap, and the depth of the $S = 3$ curve with that of spin polarization. The question of whether the periodic trends are dominated by changes in orbital overlap or spin polarization terms can then be reformulated as whether changes in the separation of the $S = 0$ and $S = 3$ states are caused primarily by shifts in the former or in the latter.

In order to obtain independent estimates of the depth of the $S = 0$ and $S = 3$ curves we clearly need to define an additional reference state in which contributions from both orbital overlap and spin polarization are negligible. The obvious reference point for a simple diatomic would be the energy of two spin-restricted atoms at infinite separation. The situation in the metal nonahalides is, however, complicated by the presence of bridging ligands, which prevent the complete dissociation of the metal ions. We therefore define a reference state corresponding to the $(a_1'\uparrow)^{0.5}(a_1'\downarrow)^{0.5}(e'\uparrow)^1(e'\downarrow)^1(e''\uparrow)^1(e''\downarrow)^1(a_2''\uparrow)^{0.5}(a_2''\downarrow)^{0.5}$ configuration (Figure 4). This state differs from the $S = 0$ state only in that it has no metal−metal bond, and from the $S = 3$ state only in that it has no spin polarization energy. The separation between the reference state and $S = 0$ therefore measures the contribution of orbital overlap (denoted ΔE_{ovlp}), while the separation between reference and $S = 3$ states (ΔE_{spe}) may be equated with the energetic contributions of the spin polarization energy. The difference between the two, $\Delta E_{spe} - \Delta E_{ovlp}$, is simply the energetic separation of the $S = 0$ and $S = 3$ states discussed above, and hence quantifies the tendency of the metal-based electrons to localize.

(31) Bauschlicher, C. W., Jr.; Walch, S. P.; Langhoff, S. R. In *Quantum Chemistry, The Challenge of Transition Metals and Coordination Chemistry*; Veillard, A., Ed.; NATO ASI Series C176; Reidel: Dordrecht, 1986; p 15.

Table 2. Overlap and Spin Polarization Energies (eV) for MCl_6 and M_2Cl_9 Complexes[a]

	ΔE_{ovlp}	ΔE_{spe}	$\Delta E_{spe} - \Delta E_{ovlp}$		single-ion SPE
$[Cr_2Cl_9]^{3-}$	+1.017	+3.547	+2.530	$[CrCl_6]^{3-}$	+1.859
$[CrMoCl_9]^{3-}$	+1.897	+2.875	+0.978		
$[Mo_2Cl_9]^{3-}$	+2.882	+2.192	−0.690	$[MoCl_6]^{3-}$	+1.144
$[MoWCl_9]^{3-}$	+2.986	+2.085	−0.901		
$[W_2Cl_9]^{3-}$	+3.096	+1.997	−1.099	$[WCl_6]^{3-}$	+1.034
$[Mn_2Cl_9]^{-}$	+0.170	+2.978	+2.808	$[MnCl_6]^{2-}$	+1.636
$[MnTcCl_9]^{-}$	+0.839	+2.338	+1.499		
$[Tc_2Cl_9]^{-}$	+1.690	+1.489	−0.201	$[TcCl_6]^{2-}$	+0.893
$[TcReCl_9]^{-}$	+1.693	+1.512	−0.181		
$[Re_2Cl_9]^{-}$	+1.846	+1.536	−0.310	$[ReCl_6]^{2-}$	+0.799

[a] See text for definition of terms.

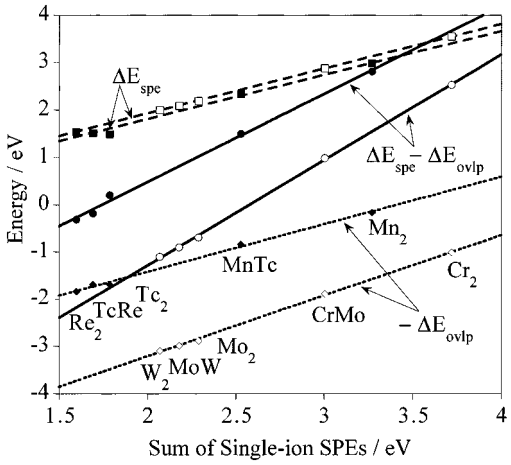

Figure 5. Variation of ΔE_{spe} (■, □), $-\Delta E_{ovlp}$ (◆, ◇) and ($\Delta E_{spe} - \Delta E_{ovlp}$) (●, ○) as a function of the sum of the single-ion spin polarization energies.[32] Complexes of the chromium triad are shown as open symbols, and those of the manganese triad are filled.

The two terms ΔE_{spe} and ΔE_{ovlp} are summarized in Table 2 for each of the 10 complexes. Spin polarization energies (SPE) for the monomeric hexachlorides, $[MCl_6]^{3-/2-}$, corresponding to the difference in energy between spin singlet $[(t_{2g}\uparrow)^{1.5}(t_{2g}\downarrow)^{1.5}]$ and spin quartet $[(t_{2g}\uparrow)^{3.0}(t_{2g}\downarrow)^{0.0}]$ states, are shown for comparison. Considering firstly the hexachlorides, we note that the spin polarization energy decreases down a triad, with the most dramatic change occurring between the first and second transition series (*ca.* 0.7 eV) compared to only a further 0.1 eV between the second and third rows. These changes are simply related to the increasing size of the ions, which in turn increases the average interelectron separation. A comparison of the complexes of the chromium triad with their isoelectronic counterparts in the manganese triad reveals that the spin polarization energy is approximately 0.25 eV lower in the latter, despite the smaller size of the M^{IV} ion. This decrease is caused by the greater covalence of the $M^{IV}-Cl$ bond, which delocalizes spin density onto the halide ions, thereby increasing the average interelectron separation.

As noted earlier, the intermediate positions of the mixed-metal systems (relative to their homobimetallic counterparts) suggest that the relative energies of the spin states of the bimetallic systems are determined largely by the sum of the contributions of the individual ions. To further test this

hypothesis, the bimetallic terms ΔE_{spe} and $-\Delta E_{ovlp}$, along with their sum $\Delta E_{spe} - \Delta E_{ovlp}$, are plotted in Figure 5 against the sum of the single-ion spin polarization energies for the octahedral monomers taken from Table 2.[32] The figure therefore links the calculated properties of the dimer to those of the component octahedral fragments.

From Table 2, there is almost a one-to-one correspondence between the ΔE_{spe} term and the sum of the single-ion spin polarization energies in both triads. This observation confirms that in the nonbonded $S = 3$ state the two metal ions are essentially independent, and the total spin polarization energy is simply the sum of the single-ion contributions. The linear dependence of the ΔE_{ovlp} term is rather more difficult to rationalize, because unlike ΔE_{spe}, ΔE_{ovlp} is dependent on the separation of the two ions. However, the data shown in Table 1 indicate that, within a triad, the equilibrium metal−metal separations in the $S = 0$ state are relatively constant, varying over a range of less than 0.15 Å. The orbital overlap term will therefore be determined principally by the radial extent of the d orbitals, which in turn is intimately related to the single-ion spin polarization energy. The approximate linear dependence of both ΔE_{spe} and $-\Delta E_{ovlp}$ on the sum of single-ion spin polarization energies dictates that a similar linear relationship must exist for the expression $\Delta E_{spe} - \Delta E_{ovlp}$. Thus the tendency of the electrons in a given complex to delocalize, as measured by $\Delta E_{spe} - \Delta E_{ovlp}$, is a linear function of the sum of the spin polarization energies of the component hexachloride monomers. Furthermore, the gradients of the $-\Delta E_{ovlp}$ and ΔE_{spe} terms in Figure 5 are very similar, indicating that the overall trend toward delocalization in the heavier complexes is caused by approximately equal changes in the orbital overlap and spin polarization energies.

A comparison of the chromium and manganese triads reveals two further significant features. Firstly, the 0.25 eV reduction in single-ion spin polarization energy for the hexachlorides of the manganese triad converts to an approximate 0.5 eV reduction in ΔE_{spe} in the dimer. Thus changes in ΔE_{spe} destabilize the $S = 3$ state in the manganese triad. Secondly, the higher positive charge on the complexes of the manganese triad causes a contraction of the metal-based orbitals relative to their counterparts in the chromium triad, thereby reducing the overlap of metal-based orbitals and destabilizing the $S = 0$ state by approximately 1.0 eV. Moving across a period, changes in ΔE_{spe} and ΔE_{ovlp} are therefore in opposition, the former favoring delocalization of the metal-based electrons, the latter localization. The 1.0 eV decrease in the ΔE_{ovlp} term dominates the 0.5 eV decrease in ΔE_{spe}, and the $S = 3$ state is stabilized by approximately 0.5 eV relative to $S = 0$ in each of the complexes of the manganese triad. This periodic trend is most clearly reflected experimentally in the longer metal−metal separation in $[Re_2Cl_9]^-$ compared to that in $[W_2Cl_9]^{3-}$.

Concluding Remarks

In this paper we have discussed the electronic structure of a series of 10 complexes of the form $[MM'Cl_9]^{3-/-}$, M = Cr^{3+}, Mo^{3+}, W^{3+}/Mn^{4+}, Tc^{4+}, Re^{4+}. The relative energies of the spin states of the mixed-metal systems are intermediate between those of their homonuclear neighbors, suggesting that the balance between localization and delocalization of the metal-based electrons is dictated primarily by the contributions of the isolated metal ions. The intermediacy of the mixed metal complexes is not, however, reflected in the ground-state metal−metal separations of the complexes, which are determined simply by which spin state lies lowest, rather than by the separation between this and higher states.

The shape of the broken-symmetry potential energy curve can be interpreted by defining three associated states, $S = 0$, 2, and 3, which have formal bond orders of 3, 1, and 0 respectively. At any particular metal−metal separation, the broken-symmetry state lies close to the lowest energy associated state, and hence the ground-state properties of any system are defined by the relative energies of the three states. For complexes containing only metals of the first transition series ($[Cr_2Cl_9]^{3-}$, $[CrMoCl_9]^{3-}$, $[Mn_2Cl_9]^-$, and $[MnTcCl_9]^-$) the $S = 3$ state always lies lowest, indicating that both σ and δ_π electrons are fully localized in the broken-symmetry ground state, leading to large metal−metal separations. At the opposite extreme, the $S = 0$ state lies lowest for the heavier complexes of the chromium triad, all metal-based electrons are delocalized, and metal−metal distances are short. The heavier complexes of the technetium triad ($[Tc_2Cl_9]^-$, $[TcReCl_9]^-$, and $[Re_2Cl_9]^-$) occupy an intermediate position where all three associated states lie relatively close in energy, indicating that the equilibrium between localization and delocalization of the electrons is finely balanced. In all three complexes a σ bond is present, but the δ_π manifold is only weakly coupled. In the ditechnetium system, the localization of the σ electrons is very facile, whereas in the dirhenium case the delocalization of the δ_π subset occurs most easily. Consequently, although the optimized structures of the gas-phase $[Re_2Cl_9]^-$ and $[Tc_2Cl_9]^-$ ions are very similar, the response of the two species to solid-state effects is likely to be very different.

The tendency of the electrons to delocalize in a given complex is governed by two distinct factors, the overlap of metal-based orbitals (favoring delocalization) and the spin polarization energy of the component ions (favoring localization). The former is related to the depth of the $S = 0$ curve, while the latter is related to the depth of the $S = 3$ curve. By defining a suitable reference state in which neither metal−metal bonding nor spin polarization is present, it is possible to obtain independent estimates of the contributions of these two factors to the equilibrium between localized and delocalized forms. On descending a triad, the metal ions become larger, causing the overlap term to increase and the spin polarization energy to decrease. Changes in both factors are found to contribute approximately equally to the stabilization of the $S = 0$ state relative to $S = 3$, and hence to the observed tendency toward delocalization in the heavier complexes. Moving across a period, the two factors are in opposition. The greater covalence of the M^{IV}−Cl bond in complexes of the manganese triad reduces the spin polarization energy by approximately 0.25 eV per metal ion, thereby favoring delocalization, but this is offset by a 1.0 eV reduction in the overlap term due to the contraction of the metal-based orbitals, favoring localization. The net result is a 0.5 eV stabilization of the $S = 3$ state relative to $S = 0$ in the manganese triad, and hence a greater tendency of the electrons to localize in these complexes.

Acknowledgment. We gratefully acknowledge the Australian Research Council (ARC) for financial support and also the Engineering and Physical Sciences Research Council, (EPSRC), U.K., for an overseas studentship to T.L.

IC961208H

(32) For example the sum of the single-ion spin polarization energies for $CrMoCl_9^{3-}$ is 1.859 eV ($[CrCl_6]^{3-}$) + 1.144 eV ($[MoCl_6]^{3-}$) = 3.003 eV.